

# Contingency analysis and identification of dynamic voltage control areas

Magesh Paramasivam, *Student Member, IEEE*, Sambarta Dasgupta, *Student Member, IEEE*, Venkataramana Ajjarapu, *Fellow, IEEE* and Umesh Vaidya, *Member, IEEE*,

**Abstract**—Contingency analysis has been an integral part of power system planning and operations. Dynamic contingency analysis is often performed with off-line simulation studies, due to its intense computational effort. Due to a large number of possible system variations, covering all combinations in planning studies is very challenging. Contingencies must be chosen carefully to cover a wider group of possibilities, while ensuring system security. This paper proposes a method to classify dynamic contingencies into different clusters, according to their behavioral patterns, in particular, with respect to voltage recovery patterns. The most severe contingency from each cluster becomes the representative of other contingencies in the corresponding cluster. Using the information of contingency clusters, a new concept called dynamic voltage control area (DVCA) is derived. The concept of DVCA will address the importance of the location of dynamic reactive reserves. Simulations have been completed on the modified IEEE 162 bus system to test and validate the proposed method.

**Index Terms**—Contingency Analysis, Delayed Voltage Recovery, Spectral Clustering, Voltage Control Area.

## I. INTRODUCTION

Contingency analysis is an important tool used to assess the security of the system under topological changes and component failures. It has been extensively used in power system planning and operation studies for deciding preventive and corrective control actions [1]. Power systems have become more complex and dynamic because of increasing penetration of renewables, operating closer to system capacity for economic benefits, increased use of electronically- controlled loads and induction motor loads. To ensure secure operation of the system, a large number of contingencies must be considered and analyzed during the planning stage. Reference [2] outlines the challenges involved in performing a contingency analysis. The large number of possible system variations pose a major difficulty in covering all combinations in planning studies. Therefore, contingencies must be chosen carefully in order to cover a wider group of possibilities, while ensuring system security.

In this paper, a method is proposed to classify contingencies into different clusters according to their behavioral patterns. The phenomenon of fault-induced delayed voltage recovery (FIDVR) is considered and the pattern in the recovery of voltages is used for the classification of contingencies. FIDVR-

related studies have received increased attention from industry and academic researchers in the recent past [3], [4]. The importance and urgency assigned to FIDVR during planning studies is directly related to the degree of induction load penetration, especially single phase air conditioning (AC) in the system. Increasing efforts have been made to properly represent the behavior of induction motor loads in planning studies [5]. FIDVR is one of the emerging issues that might affect the reliability of the future grid [6]. The U.S. Department of Energy (DOE) Workshops on FIDVR recognized the growing concerns of utilities over FIDVR events and considers it a national issue because of the increasing penetration of residential AC loads [7], [8]. The DOE is sponsoring FIDVR research activities to promote national awareness among utilities, improve understanding of potential grid impacts, and identify appropriate steps to ensure reliability of the power system [3]. The major cause for FIDVR events is related to the dynamic behavior of induction motor loads, which tend to decelerate and stall, following a large disturbance, resulting in low voltages in a significant portion of the power system. The reactive requirement of the induction motor increases when the induction motor stalls and may prevent quick voltage recovery. While the disturbance leading to FIDVR problems may be initiated by different kinds of contingencies, the underlining problem is an inherent weakness in the power system (lack of dynamic VAR support). Contingencies in a particular region affect a certain set of buses and expose the weakness in the system. This work propose to group the contingencies that produce similar response in terms of voltage behavior using clustering procedure. If the contingencies that create similar effect on the system are grouped together then instead of considering all contingencies only severe contingency can be considered for further analysis and planning studies.

In this paper, FIDVR is characterized using a statistical measure called Kullback-Liebler (KL) divergence measure. This characterization is used to define the similarity between contingencies and the spectral clustering algorithm is employed to identify the contingency clusters. Then, the most influential buses for dynamic VAR injections are found by sensitivity studies for the identified severe contingencies. Using the information of contingency clusters and the most influential buses, a new concept called dynamic voltage control area (DVCA) is derived. The concept of DVCA will address the importance of the location of dynamic reactive reserves. Identification of effective dynamic VAR support locations to reduce the risk of FIDVR events is one of the important

Authors are with the Department of Electrical and Computer Engineering Iowa State University, Ames, Iowa 50011. U. Vaidya and S. Dasgupta would like to acknowledge financial support from the National Science Foundation CAREER grant ECCS 1150405 and PSERC grant S-50. Email: mageshp@iastate.edu, dasgupta@iastate.edu, vajjarap@iastate.edu and ug-vaidya@iastate.edu

factors identified by NERC planning committee while dealing with FIDVR studies. Utilities such as Southern California Edison (SCE), Arizona public services (APS), Center Point Energy, Georgia Transmission Company have installed static var compensator (SVC) in their system to provide dynamic VAR support [3]. This work attempts to develop a systematic approach to identify the different areas experiencing short term voltage problems and identify the effective dynamic VAR support locations using the concept of DVCA. A DVCA is defined as a section of a power system that responds as a cohesive unit to avoid short-term voltage stability problems within that section. For example, given a voltage deviation within a DVCA, the dynamic reactive resources within that area respond together to prevent short-term voltage stability problems in this area. As long as minimum levels of dynamic reactive reserves are maintained in each area, then the likelihood of occurrence of short-term voltage stability problems will be minimized.

The paper is organized as follows: Section II briefly describes the characterization of FIDVR using the KL divergence measure. Section III describes the procedure involved in contingency clustering. Section IV provides the concept of dynamic voltage control areas. Simulation studies based on the modified IEEE 162 bus system have been provided in Section V. Conclusions are provided in section VI.

## II. CHARACTERIZATION OF FIDVR

In this section, the key results from [9] for the characterization of FIDVR using KL measure are presented from a rigorous analysis and detailed description provided in [9]. To characterize the FIDVR phenomenon, KL divergence, an entropy-based measure is utilized. Characterization of voltage waveforms using the KL measure will quantify FIDVR in a scalar quantity and also be helpful in comparing different voltage recoveries. The KL divergence is a popular measure of distances used in statistics and information theory [10],[11]. The major steps involved in calculating the KL divergence for voltage waveforms are outlined below.

Step 1) The voltage axis is partitioned into  $N$  subintervals. The voltage samples are observed from fault clearing instant to the final observation time. The number of voltage samples in each subinterval is counted. This number provides information about the time the voltage waveform is present in a subinterval.

Step 2) The number of samples in a particular subinterval is divided by the total number of samples to obtain the normalized subinterval frequency. This generates the probability density function of the given voltage waveform. Figure 1 (a) shows a slow recovering voltage waveform and the blue colored bars in Fig. 1(b) is the corresponding probability density function.

Step 3) Construct the probability density function for the reference voltage recovery using (1).  $y_i$  refers to the  $i^{th}$  partition of the voltage axis and corresponds to the voltage level,  $v_i$ . The parameter,  $\lambda$ , controls the width of the reference probability distribution concentrated around the nominal voltage level,  $v_{nom}$ . The normalizing factor,  $Z$ , makes the

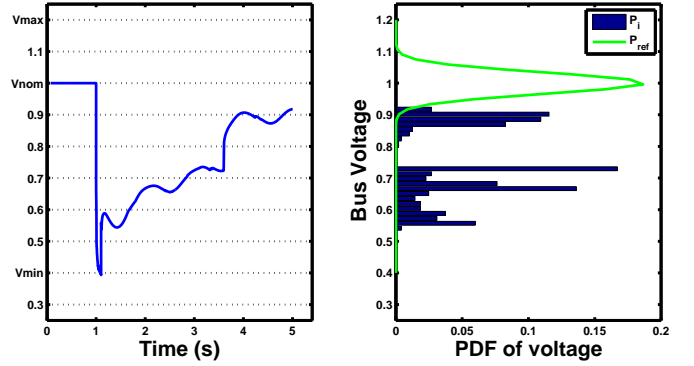


Fig. 1. (a) Voltage time series for  $KL=16.7$  (b) Probability density function for the voltage series in part (a) and ideal voltage recovery.

summation of the reference distribution equal to 1.

$$p_{ref,i} := \frac{e^{-\lambda(y_i - v_{nom})^2}}{Z}, \quad i = 1, 2, \dots, N. \quad (1)$$

$$Z = \sum_{i=1}^N e^{-\lambda(y_i - v_{nom})^2}$$

Step 4) Calculate the KL divergence measure using (2a). This is the relative entropy between two probability density functions,  $p$  and  $p_{ref}$ , denoted by  $K(p||p_{ref})$ . The KL divergence can be further simplified to (2b).

$$K(p||p_{ref}) = \sum_{i=1}^N p_i \ln \frac{p_i}{p_{ref,i}} \quad (2a)$$

$$\mathcal{K} = \ln Z + \sum_{i=1}^N p_i \ln p_i + \lambda \sum_{i=1}^N p_i (y_i - v_{nom})^2 \quad (2b)$$

The value of KL is bounded below by zero and will be zero only when the probability distribution generated by the voltage waveform exactly matches the reference probability distribution,  $p_{ref}$ .

The critical value of KL for a general specification of voltage performance as given in (3) is derived. If the value of KL is greater than this critical value, then this implies voltage performance violations. On the other hand if the value is less than the critical KL, there can be two possibilities (1) there are no violations (2) the violations are very small and not severe.

$$\begin{aligned} v(t) &\geq V_1, \quad T_{cl} \leq t < T_1, \\ v(t) &\geq V_2, \quad T_1 \leq t < T_2, \quad V_2 > V_1, \\ v(t) &\geq V_3, \quad T_2 \leq t \leq T_f, \quad V_3 > V_2, \end{aligned} \quad (3)$$

where  $T_{cl}$  denotes the fault clearing time and  $T_f$  denotes the final time period.

If the voltage time series satisfies the performance conditions mentioned in (3), then the corresponding KL divergence has the following upper bound,

$$\begin{aligned} \mathcal{K}^* &:= \frac{1}{\Delta T_f} (\Delta T_1 \log \Delta T_1 + \Delta T_2 \log \Delta T_2 + \Delta T_3 \log \Delta T_3) \\ &+ \frac{\lambda}{\Delta T_f} (\Delta T_1 (V_1 - V^*)^2 + \Delta T_2 (V_2 - V^*)^2, \\ &+ \Delta T_3 (V_3 - V^*)^2) + \log Z - \log \Delta T_f \end{aligned} \quad (4)$$

where  $\Delta T_1 := T_1 - T_{cl}$ ,  $\Delta T_2 := T_2 - T_1$ ,  $\Delta T_3 := T_f - T_2$  and  $\Delta T_f := T_f - T_{cl}$ .

The WECC performance criteria state that following an N-1 contingency, the voltages at all load and non-load buses should not exceed its nominal voltage by 25 and 30%, respectively. Also, the criteria state the voltage at load buses should not exceed their nominal value by 20% for more than 20 cycles. For the voltage bounds specified by the Western Electricity Coordinating council (WECC) voltage performance criteria [12], the value of the KL measure is calculated as 4.9 with parameters  $\lambda = 450$  and  $N = 50$ .

In this paper, the KL value calculated with the above mentioned parameters and WECC performance criteria boundary conditions is treated as a critical KL value. A value of the KL measure above this critical value implies violations in the performance criteria. The higher the value of the KL measure, the more severe the violation of WECC performance criteria at the corresponding bus. When the value of the KL measure is below 4.9, this implies the voltage signal recovers fast and also settles within the bounds specified by WECC performance criteria.

### III. CONTINGENCY CLUSTERING

In the planning studies, analyzing all combinations is a computationally challenging problem, due to the large number of possible system variations. To alleviate this problem, only the most severe contingencies are selected, based on certain performance criteria. However, it is possible the problems caused by the most severe contingencies are confined to a certain region and there might be relatively less severe contingencies that create problems in different regions of this system. The focus of this work is to select the most important contingencies from a given set of input contingencies, for analysis in the planning stage. First, the clustering-based approach to identify severe contingencies for a given operating condition is presented. Given a power system with  $N_B$  buses and a set of  $N_C$  possible N-1 contingencies, the goal is to identify sets of contingencies such that contingencies in the same set would produce similar patterns of response in the system. Then a framework for selecting the representative contingencies from a wide range of operating conditions is provided at the end of this section. The input set of contingencies,  $N_C$ , can be selected based on the operators knowledge about the system, past experiences, most probable contingencies, contingencies of severe type etc.

#### A. Similarity of Contingencies

Using the time domain simulation results, KL divergence at each bus is computed for all contingencies and the results are stored in a matrix  $\bar{K} \in \mathbb{R}^{N_B \times N_C}$ . The element  $\mathcal{K}_{ij}$  of the  $\bar{K}$  matrix has the summarized information of the voltage time series corresponding to the  $i^{th}$  bus and  $j^{th}$  contingency in a scalar form. Let  $U_i$  and  $V_j$  denote the  $i^{th}$  row and  $j^{th}$  column of  $\bar{K}$ .  $U_i \in \mathbb{R}^{N_C}$  contains the KL divergence for the  $i^{th}$  bus for all contingencies and  $V_j$  contains the KL divergence for all buses for the  $j^{th}$  contingency. Numerous measures, such as Euclidean distance, cosine similarity, Pearson and Spearman rank correlation (SC), are available to describe the similarity

between two vectors. However, for defining the similarity between the two contingencies it has been found that the SC yields better results compared to other measures because it measures the monotone relationship between the KL vectors corresponding to different contingencies. For computing the SC value, first the KL measure of the two contingencies provided in  $V_{j_1}$  and  $V_{j_2}$  are converted to rank vectors,  $R_{j_1}$  and  $R_{j_2}$ , respectively. The bus corresponding to the lowest KL value is assigned the least rank (rank 1) and the bus corresponding to highest KL value is assigned the highest rank (rank N). When there are identical KL values in a contingency vector, then a rank equal to the average of their positions in the ascending order of values is assigned to the buses corresponding to rank ties. The rank vectors are used to compute the Spearman correlation using (5).

$$r_s := \frac{\sum_{k=1}^{N_B} (R_{j_1}(k) - \bar{r}_{j_1})(R_{j_2}(k) - \bar{r}_{j_2})}{\sqrt{\sum_{k=1}^{N_B} (R_{j_1}(k) - \bar{r}_{j_1})^2 \sum_{k=1}^{N_B} (R_{j_2}(k) - \bar{r}_{j_2})^2}}, \quad (5)$$

$$\text{where } \bar{r}_{j_1} := \frac{1}{N_B} \sum_{k=1}^{N_B} R_{j_1}(k), \quad \bar{r}_{j_2} := \frac{1}{N_B} \sum_{k=1}^{N_B} R_{j_2}(k),$$

$r_{j_1}$  and  $r_{j_2}$  denotes the mean values of rank vectors corresponding to contingencies  $j_1$  and  $j_2$ , respectively.

The Spearman rank correlation,  $r_s$ , works on the ranks of two vectors, instead of the actual data provided in the vectors. It takes values between +1 and -1. When  $r_s$  takes the value of 1, it indicates a perfect association of ranks between the two contingencies and a value of -1 indicates a perfect negative association of ranks (highest ranked bus in contingency 1 becoming lowest rank in contingency 2 and vice versa). A value of  $r_s$  close to zero signifies a weak association between ranks of the two contingencies.

#### B. Spectral Clustering Algorithm

A spectral clustering technique [13] is utilized to group the contingencies into different clusters based on the similarity information. The Spearman rank correlation is used to define the similarity between contingencies. The following steps describe the algorithmic procedure involved in grouping contingencies using spectral clustering technique.

Step 1) Pre-processing: This step chooses the set of contingencies and buses that must be considered for further analysis. When the affected region is very small compared to the total number of buses, the computed correlation will lead to misleading similarity information between the two contingencies. Therefore, neglecting non-severe contingencies and buses will improve the accuracy of the results. The threshold values to determine severe contingencies and buses from non-severe cases are system and user dependent. The threshold values for the selection of contingencies and buses are provided as an input to the cluster analysis.

Step 2) Similarity matrix (S): The similarity matrix defines the distance between each contingency with respect to all other contingencies. First, compute the SC between two contingencies,  $j_1$  and  $j_2$ , using (5). Then, the SC values are converted into the distance measure by using the transformation  $d_{j_1 j_2} = 1 - r_s^{j_1 j_2}$ . The value of  $d_{j_1 j_2}$  provides the distance

measure between the two contingencies,  $j_1$  and  $j_2$ . If the two contingencies affect similar buses in the same rank order, then the corresponding correlation value will be close to 1 and the distance between them is close to zero. If the SC value is -1, then the distance will have a value of 2, indicating dissimilarity between the two contingencies. Since the SC value lies in the range of -1 and 1, the distance measure will lie in the range of 0 to 2.

Step 3) Adjacency matrix (A): Calculate the adjacency matrix (A) using a Gaussian similarity function as shown in (6a). The parameter,  $k_p$ , scales the similarity function value and  $\sigma$  is the connectivity parameter, which defines the extent of similarity between two contingencies. The degree matrix, D, is a diagonal matrix with entries  $s_1, \dots, s_j, \dots, s_{RC}$ , as defined in (6b), along its diagonal.

$$A_{j_1 j_2} = k_p e^{-\frac{d_{j_1 j_2}}{\sigma}}, \quad A_{j_2 j_1} = A_{j_1 j_2}, \quad j_1 \neq j_2, \text{ and} \quad (6a)$$

$$s_j = \sum_{k, k \neq j}^{N_{RC}} A(j, k), \quad A \in \mathbb{R}^{N_{RC} \times N_{RC}}. \quad (6b)$$

$N_{RC}$  denotes the reduced number of contingencies that have been obtained after the pre-processing step.

Step 4) Calculate the graph Laplacian matrices using (7). Matrix  $L$  and  $L_{\text{norm}}$  represent the unnormalized and normalized graph Laplacian matrix, respectively.  $L_{\text{norm}}$  is a positive semi-definite matrix and have  $N_{RC}$  non-negative real valued eigenvalues,  $0 = \lambda_1 \leq \dots \leq \lambda_{N_{RC}}$ .

$$\begin{aligned} L &= D - A. \\ L_{\text{norm}} &= D^{-\frac{1}{2}} L D^{\frac{1}{2}}. \end{aligned} \quad (7)$$

Step 5) Identify the preliminary number of clusters using the eigenvalues analysis on the Laplacian matrix. If the eigenvalue, 0, has a multiplicity of  $k$ , this implies there are  $k$  fully disconnected clusters. However, this is an ideal scenario and does not happen in power systems. There are a number of methods available in the literature for choosing the initial number of clusters,  $k$ , for the clustering algorithm. Of the available methods, the eigengap heuristic is used to identify the initial number of clusters, where the goal is to identify the number,  $k$ , such that all eigenvalues,  $\lambda_1, \dots, \lambda_k$ , are small, but  $\lambda_{k+1}$  is relatively large.

Step 6) Compute the first  $k$  eigenvectors,  $e_1, \dots, e_k$ , of normalized graph Laplacian matrix,  $L_{\text{norm}}$ .

Step 7) Form the matrix  $E \in \mathbb{R}^{N_{RC} \times k}$  using the first  $k$  eigenvectors,  $e_1, \dots, e_k$ , as columns. Let  $y_j \in \mathbb{R}^k$ ,  $j = 1, \dots, N_{RC}$  be the vector corresponding to the  $j$ -th row of  $E$ .  $y_j$  denotes the  $j^{\text{th}}$  contingency from the reduced contingency list in the lower dimensional space. The key aspect of the spectral clustering algorithm is to change the representation from abstract data points  $V_j$  in higher dimensional space to  $y_j$  in lower dimensional space. The change of representation enhances the cluster properties in the data so the clusters can be identified easily in the new representation, using K-means clustering.

Step 8) Cluster the points,  $y_j$ , using K-means algorithm into different clusters,  $C_1, \dots, C_k$ . The K-means algorithm

partitions the data points,  $y_j$ , in the matrix,  $E$ , into  $k$  clusters. The K-means algorithm identifies the clusters, such that it minimizes the sum of the distance for each data point in the cluster to the centroid of the corresponding cluster.

Step 9) For each identified cluster, recompute the Laplacian matrix with contingencies belonging to the corresponding cluster. Checking further clustering is possible by investigating the dominant eigenvalues of the new Laplacian matrix. If further clustering is possible, repeat the clustering algorithm from Step 5. If further clustering is not possible, stop the clustering algorithm and provide the final results.

A result of contingency clustering is contingencies that produce similar behavioral patterns in system voltage response are grouped together in different clusters. The most severe contingency in each cluster will act as a representative for all other contingencies in the corresponding cluster. Only these representative contingencies, which represent all other contingencies, are considered for further analysis. Also, the cluster analysis provides the most severely affected buses corresponding to each cluster. The application of clustering based on similarity information reduces the complexity of planning problem, especially when dealing with large scale system. Also, this approach provides a systematic way to reduce the complexity of dealing with multiple contingencies.

### C. Contingency Clustering - Multiple operating conditions

The power system undergoes continuous variation in loads, generation and system configuration. This presents a large number of scenarios that have to be taken care of during planning stage. The scenarios (operating conditions, load levels, contingencies) have to be chosen carefully such that it covers a wider group of possible cases. The clustering procedure described in section III-B can be extended to reduce the number of scenarios to be analyzed.

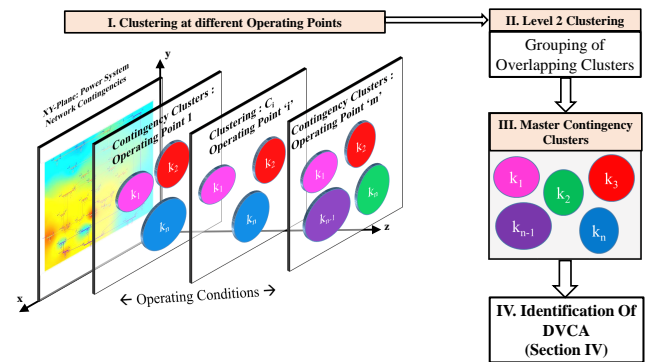


Fig. 2. Contingency clustering framework for multiple operating conditions

Figure 2 provides the framework for handling multiple scenarios and operating conditions in the process of DVCA identification. First, the clustering of contingencies is performed at different operating conditions. Second, the resulting clusters are further grouped based on their similarity. Numerous measures such as rand index, mirkin distance, Jaccard index, variation of information (VOI) are available to compare the similarity between clusterings. A clustering,  $C_i$ ,

is a group of contingency clusters at one operating condition. The variation of information (VOI) metric calculated by (8a) is used to find the similarity between clusterings [14].  $H(C_i)$  is the entropy associated with clustering of contingencies at operating condition,  $i$  and is computed using (8b).  $K_i$  and  $K_j$  denotes the total number of clusters in clusterings  $C_i$  and  $C_j$  respectively. The number of contingencies in the  $k^{th}$  cluster in clustering  $C_i$  is denoted as  $n_{k_i}$  and  $N_c$  represents the total number of input contingencies.  $I(C_i, C_j)$  has the mutual information between the clusterings  $C_i$  and  $C_j$ . The VOI metric measures the amount of information lost and gained in forming clustering  $C_j$  from  $C_i$ . Consequently, lower values of VOI implies better similarity between the clusterings.

$$VOI(C_i, C_j) = H(C_i) + H(C_j) - 2I(C_i, C_j), \quad (8a)$$

$$VOI \in [0 \log N_c]$$

$$H(C_i) = - \sum_{k_i=1}^{K_i} P(k_i) \log P(k_i), \quad (8b)$$

$$I(C_i, C_j) = \sum_{k_i=1}^{K_i} \sum_{k_j=1}^{K_j} P(k_i, k_j) \log \frac{P(k_i, k_j)}{P(k_i)P(k_j)} \quad (8c)$$

$$P(k_i) = \frac{n_{k_i}}{N_c}, \quad P(k_i, k_j) = \frac{|C_{k_i} \cap C_{k_j}|}{N_c} \quad (8d)$$

The VOI metric can be normalized by its maximum value ( $\log N_c$ ) and can be used as the distance metric to compute the graph Laplacian matrix (Refer Sec. III-B). Utilizing the eigenvalue analysis of this Laplacian matrix, k-means clustering is performed to group the similarly behaving clusterings. The representative contingencies from different groups of clusterings forms the final contingency set that is used for the identification of DVCA.

#### IV. DYNAMIC VOLTAGE CONTROL AREAS

Reference [15] describes a method to identify voltage control areas based on steady state analysis. This method uses the PV curve tracing method to push the system to the point of instability for all considered contingencies. For each considered case, modal analysis is performed at the point of instability to identify the critical modes of instability. Based on the participation factors (PFs) of buses corresponding to the critical mode, data mining techniques are employed to identify contingency clusters and the voltage control area (VCA). The measure used for contingency clustering is similarity in PFs. Generators that have high PFs are chosen as the initial set of control candidates to represent each contingency cluster. The PFs corresponding to zero eigenvalue (critical mode) indicate the buses contributing to the instability. In this work for identifying DVCA, the KL measure is used to define the similarity between contingencies (Refer section:III-A). The KL measure indicates the relative participation of buses contributing to short-term voltage problems. Figure 3 provides the important steps involved in the process of identifying DVCA.

Step 1) Clustering of contingencies: Groups of contingencies behaving similarly are identified through the clustering

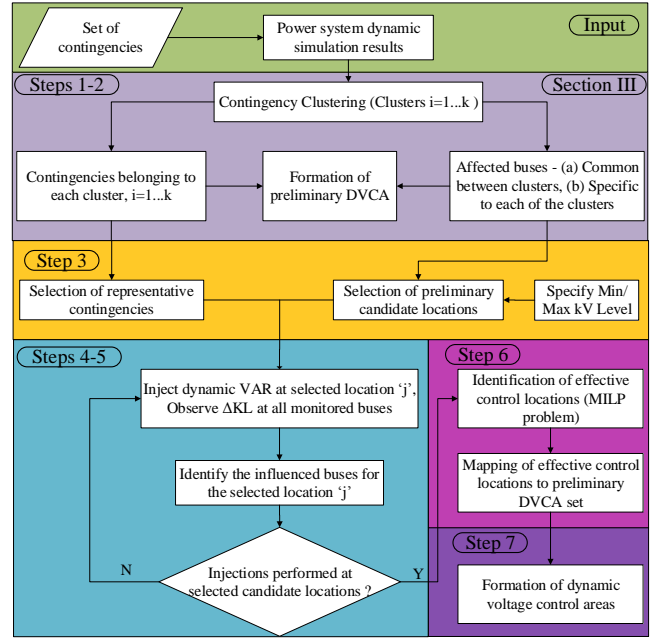


Fig. 3. Overview of steps involved in the identification of dynamic voltage control areas

procedure (Refer Section III-B). The most severe contingency from each cluster is a representative of all other contingencies in the corresponding cluster. Only the representative contingencies are chosen for further analysis.

Step 2) Identification of affected buses: For each cluster, all buses with violations of performance criteria form the set of violated buses corresponding to the cluster. Among the violated buses, some buses are affected only by contingencies specific to a particular cluster and some buses are affected by contingencies belonging to different clusters. The affected buses are grouped into different sets, such as specific to each clusters and common between clusters through a hierarchical clustering procedure. The number of common affected buses between clusters is used as the similarity measure for the hierarchical clustering procedure.

Step 3) Identification of preliminary DVCA: Each set of affected buses along with its corresponding contingency clusters form the preliminary DVCA. The contingency clusters provide the group of contingencies that result in the violations in the buses belonging to its DVCA. For example, if the set of affected buses correspond to buses common to two clusters, then contingencies corresponding to these two clusters have influence on this set of buses.

Step 4) Identification of potential control candidate locations: In the DVCA identification procedure, one of the challenges is to identify the initial control candidate locations, which are effective locations for placing dynamic reactive resources. Placement of dynamic VAR devices, such as SVC and STATCOM, at lower kV levels is relatively cheap, but it will not help wider range of buses in the system. On the other hand, placing them at higher kV levels helps a wider range of buses to improve their voltage levels, but is very costly. Therefore, based on economic considerations, the loads buses between the specified minimum and maximum kV levels are

chosen as preliminary candidate locations.

Step 5) Sensitivity studies: The influence of potential control candidate locations is identified through sensitivity studies. The trajectory sensitivity index (TSI) is used in [16] to identify the relative effectiveness of locations for placing dynamic VAR sources. Similar to TSI, sensitivities to the KL measure are used to capture the effectiveness of selected candidate locations. For the representative contingencies, the change in KL measures at all monitored buses to injection of dynamic VARs at the chosen candidate locations are calculated.

Step 6) Identification of effective control locations: The effective control locations are identified by a mixed integer linear programming (MILP) problem utilizing the KL sensitivities from Step 5. The constraints of the MILP include the specified performance criterion on KL values at all monitored buses and limitations on the maximum amount of reactive sources that can be placed at each location. Details of the MILP problem are provided in section IV-A. The MILP identifies the effective control locations and amount of dynamic VARs required to meet the specified KL performance criteria, considering the representative contingencies from cluster analysis.

Step 7) Identification of DVCA: The effective control locations identified by the MILP problem are mapped to its corresponding preliminary DVCA set. The mapping results in effective control locations that influence a set of affected buses for a given set of contingencies. After mapping, if a preliminary DVCA set does not have any control locations, then it is merged with its corresponding common preliminary DVCA sets. The area of influence of control candidate locations are identified from the sensitivity study results. For injection of dynamic VARs at a control location, the buses that produced a change in the KL value above a certain specified threshold value form the area of influence for the corresponding control location. Each resulting group with a set of contingencies, affected buses, and effective control locations forms a DVCA.

#### A. Mixed Integer Linear programming problem for finding effective control locations

Sensitivity studies with different levels of dynamic reactive power injection are performed to identify the influence of VAR injections on the KL measure at different buses. The results of sensitivity studies are utilized to formulate the MILP optimization problem. The general formulation of the MILP optimization problem for handling multiple contingencies is provided in (9).

The parameters,  $C_B^i$ ,  $C_{Q_{ml}}^i$ , denote the fixed cost and variable cost respectively, based on the size of the dynamic VAR device at location  $i$ . The status of the integer variable,  $B^i$ , determines the selection of location  $i$  for dynamic VAR placement. The variable,  $Q_{ml}^i$ , provides the amount of dynamic VAR device required at location  $i$  for contingency  $m$  and level  $l$ . The integer,  $W_{ml}^i$ , is an indicator variable that indicates whether  $Q_{ml}^i$  has reached its corresponding range limit,  $Q_{ml}^{R,i}$ . The maximum capacity of the dynamic VAR device at a particular location is given by  $Q_{ml}^{i,max}$ . The constants,  $N_{cont}$ ,  $N_{lev}$ ,  $N_{Loc}$ , define the number of contingencies, the number of levels used for dynamic VAR injection in sensitivity studies, and

the number of initial candidate locations, respectively. Sets SMon and SCont define the sets of monitored buses and contingencies, respectively.

$$\text{minimize}_{B,Q} F = \sum_i^{N_{Loc}} C_B^i B^i + \sum_m^{N_{cont}} \sum_l^{N_{lev}} \sum_i^{N_{Loc}} C_{Q_{ml}}^i Q_{ml}^i,$$

Subject to

$$(C1) : \sum_j^{N_{Loc}} \frac{\partial K^i}{\partial Q_{ml}^j} Q_{ml}^j \leq K^* - K_{m,i}^{(0)}, \quad (9)$$

$$(C2) : \sum_l^{N_{lev}} Q_{ml}^i \leq B^i Q_{ml}^{i,max},$$

$$(C3) : Q_{ml}^{R,i} W_{ml}^i \leq Q_{ml}^i \leq Q_{ml}^{R,i} W_{m(l-1)}^i, \\ \forall i \in \text{SMon}, \forall m \in \text{SCont},$$

$$B \in \{0, 1\}, Q \in \mathbb{R}^{N_{Loc}}, W \in \{0, 1\}$$

The objective of this MILP formulation is to identify effective control candidate locations and the minimum amount of dynamic reactive power needed to meet the required performance constraints (set C1). The performance constraints include the KL divergence measure at the monitored buses should be less than the critical value of the KL divergence measure for all the contingencies. For contingency  $m$ ,  $K_{m,i}^{(0)}$  is the base case KL measure at location  $i$ .  $K^*$  denotes the critical value of the KL divergence measure based on WECC performance criteria (Refer section II). The constraints set C2 provide limits to the maximum amount of dynamic VAR placed at a given location. The constraints set C3 is included to preserve the linearity of the optimization formulation.

## V. SIMULATION RESULTS

Simulations have been performed in IEEE 162 bus system. The test system has 17 generators, 111 loads, 34 shunts, and 238 branches. The power flow and dynamics data for the 162 bus system are available in [17]. The total generation capacity and load of the system are 20.60 GW and 17.27 GW respectively. For a more accurate load representation, 22 load buses were stepped down through distribution transformers to the 12.47 kV level, and the new low voltage buses were assigned the numbers 163 through 184. **Dynamic simulation studies are performed using PSSSE software [18]. To capture the dynamic behavior of motor loads, a composite load model represented by CMDL was used at the new representative load buses.** Additionally, composite load models were also used to represent motor loads at the major load centers (zones 3 and 6). Of the total load for each bus, 30% is specified as three-phase induction motor loads and 35% as single-phase air conditioner loads.

The modified IEEE 162 bus system has  $N_B$  buses (184) and a total of  $N_C$  contingencies (316) of the type, a three-phase fault at a bus cleared after 6 cycles by opening one of the transmission lines connected to the faulted bus is considered for simulation studies. The voltage time series corresponding to bus  $i$  and contingency  $j$  are stored in the vector,  $v_{ij}(t)$ ,  $0 \leq t \leq T_f$ ,  $i \in N_B$ ,  $j \in N_C$ .  $T_f$  represents the final simulation

time instant chosen as 5 seconds for all the simulations.

In the pre-processing step, only those contingencies affecting more than 5% of the total number of buses are considered for further analysis. This reduces the number of contingencies from 316 to 71. Also, the KL values for buses that do not have violations for more than 10 contingencies are discarded for further analysis. A more detailed analysis and discussion on the severity of contingencies and buses are provided in [9]. After the pre-processing step, the  $\bar{K} \in \mathbb{R}^{N_B \times N_C}$  has been reduced to  $\bar{K} \in \mathbb{R}^{70 \times 71}$ .

The correlation matrix, as plotted in Fig 4, shows the correlation values between different contingencies, where the rows and columns represent the contingency identification numbers (cIDs) in the reduced contingency list. The different colors in the matrix plot corresponds to SC values as indicated along the sidebar in fig 4. When the correlation value is close to 1, the matrix block has shades of red signifying the strong similar behavior between the cIDs given by the row and column number (e.g. cIDs 4 and 5). Similarity signifies both the contingencies affect the same set of buses in the same rank order based on the KL values. When the correlation value decreases below 0.6, then the contingencies exhibit weak correlations. When the correlation value become negative, the matrix block has shades of blue, signifying dissimilarity between these corresponding contingencies (e.g. cIDs 1 and 32). Dissimilarity signifies buses severely affected by one contingency are not affected by another contingency.

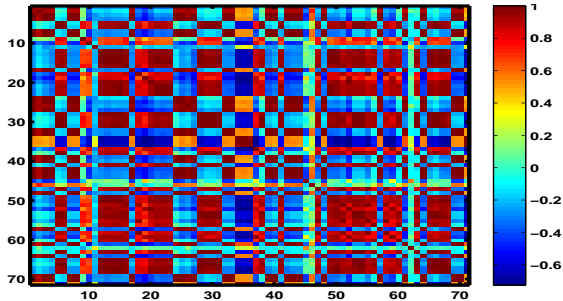


Fig. 4. Plot of Spearman's rank correlation between all contingencies. Rows and columns represent indices of different contingencies.

The SC values between contingencies are converted into distance between contingencies using the transformation provided in Step 2 of section III.B. Strongly correlated contingencies will have a distance close to 0 and weakly correlated contingencies will have a distance close to 2. Since the correlation between contingencies changes from strong to weak, the corresponding distance between them increases from 0 to 2. The distance between contingencies is used to compute the adjacency matrix utilizing a Gaussian similarity function. The computed adjacency matrix using (6a) will have values in the range of 0 to 1. A value of 1 in the adjacency matrix implies contingencies belonging to corresponding row and column are adjacent and belong to the same group of contingency cluster. If the adjacency value between two contingencies is close to 0, then it implies they are dissimilar and belong to a different contingency cluster. The goal of the clustering

algorithm is to group contingencies with adjacency values close to 1 with respect to each other. Such groupings will result in contingencies that create a similar voltage response in the system placed in the same cluster.

Figure 5 shows the eigenvalue plots for the analysis of 71 contingencies. From the eigenvalue analysis of the normalized Laplacian matrix, the preliminary number of clusters is 2. The first two eigenvectors of the matrix  $L_{norm}$  are used to represent the similarity data in a reduced dimensional space. K-means clustering algorithm is performed using the number of clusters and corresponding eigenvector data. The distance measure used by the K-means algorithm is city block distance. Figure 6 shows the plot of the second eigenvector after rearranging the rows based on K-means cluster results. If the eigenvector 2 is thresholded at -0.05, then the part below -0.05 corresponds to cluster 1 and the part above -0.05 corresponds to cluster 2. Each data point in Fig. 6 corresponds to a contingency ID. The number of contingencies in the two different clusters are 29 and 42.

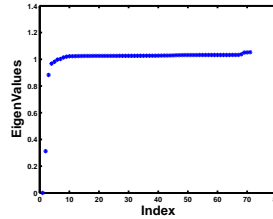


Fig. 5. Plot of eigenvalues

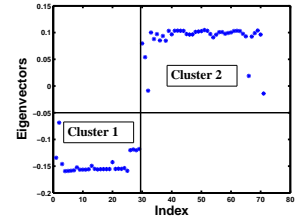


Fig. 6. Plot of eigenvectors

When the correlation information between the contingencies is placed in random order as shown in Fig. 4, the presence of clusters is difficult to discern. However, after clustering analysis, the two clusters, shown by red colored regions along the diagonal of the adjacency matrix, are clearly separated in Fig. 7. The shades of red imply contingencies have strong similar behavior with respect to the other contingencies in the same cluster and shades of blue imply their separation from contingencies in other clusters. There are 29 contingencies in cluster 1 and 43 contingencies in cluster 2, as indicated in Fig. 7. The contingencies are ordered such that the most severe contingency in a cluster is placed first and the least severe contingency is placed last. For example, cIDs 1 and 30 are the most severe contingencies in clusters 1 and 2, respectively. Similarly, cIDs 29 and 71 are the least severe contingencies in clusters 1 and 2, respectively. The first 24 contingencies in cluster 1 exhibit strong similar behavior with respect to each other, whereas cIDs 25-29 exhibit a strong similarity among themselves, but relatively weak similarity with respect to the other contingencies in the cluster. This is due to the fact these five contingencies are less severe and affect only a subset of buses affected by the most severe contingency in cluster 1. It can be also noted these contingencies exhibit a strong dissimilarity with contingencies in cluster 2. Similarly, a few contingencies in cluster 2 exhibit a weak correlation with other contingencies in cluster 2, but they have a strong dissimilarity with cluster 1 contingencies.

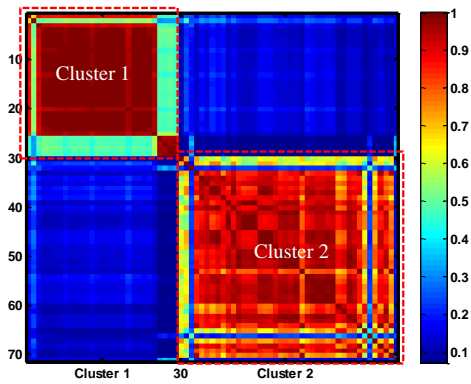


Fig. 7. Plot of Adjacency Matrix - After clustering. Rows and columns represent rearranged indices of different contingencies.

### A. Validation of Clustering Results

Cluster validity refers to the procedure of evaluating the results of the clustering technique. In this paper, validation is accomplished using internal criteria of validating clustering procedure. With respect to the internal criteria, the two commonly used measures for validating clustering results are compactness and separation. Compactness measures the closeness of contingencies within a cluster and separation measures how distinct or well separated a cluster is from other clusters. A silhouette coefficient combines the idea of both cohesion and separation for clusters and clusterings [19]. Silhouette values help interpret cluster results and provide a graphical representation of how well each object lies within its cluster. The silhouette value for the  $i^{\text{th}}$  data point,  $s(i)$ , is calculated by using the formula,  $s(i) = \frac{b(i) - a(i)}{\max\{a(i), b(i)\}}$ . The average dissimilarity of  $i^{\text{th}}$  contingency with all other contingencies within the same cluster is denoted by  $a(i)$ . The average dissimilarity of the  $i$  with contingencies of other clusters where contingency  $i$  is not a member is calculated and the lowest dissimilarity is denoted as  $b(i)$ . The city block distance measure, as used in k-means clustering, is used to define the dissimilarity. The value of  $a(i)$  defines how well the contingency,  $i$ , is related to the cluster it belongs. When the value of  $a(i)$  is smaller, the matching of contingency  $i$  to its assigned cluster is better. The value of  $b(i)$  defines how well contingency  $i$  is separated from other clusters. The larger the value of  $b(i)$ , the poorer is the matching of contingency  $i$  to the other clusters. The value for  $s(i)$  lies between -1 and 1. When the value of  $a(i) \ll b(i)$ , then the value for  $s(i)$  will be close to 1. A value of  $s(i)$  close to 1 signifies the corresponding contingency is properly clustered. When the value of  $s(i)$  is close to 0, then the contingency is on the border line between two clusters. When the value of  $s(i)$  is close to -1 signifies a misclassification of the contingency.

For illustration of clustering validation, sample plots of silhouette values for two different numbers of clusters ( $k=2$  and 4) are shown in Figs. 8 and 9. The average silhouette value for clustering with  $k$  as 2 and 5 are determined 0.8739 and 0.6039, respectively. The higher the value of the average silhouette value, the better the clustering result. When the value of  $k$  is specified as 4, some of the silhouette values become negative, indicating the contingencies are improperly

clustered.

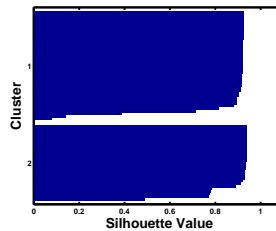


Fig. 8. Silhouette plot for clustering with  $k=2$ . Average Silhouette value is 0.8739

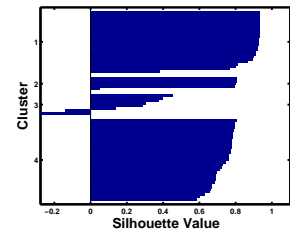


Fig. 9. Silhouette plot for clustering with  $k=4$ . Average Silhouette value is 0.6039

The silhouette value can be used to provide the natural number of clusters within a data set and compare the two different clusterings. The average silhouette value over the entire data set provides a measure of how appropriately the contingencies have been clustered. An average silhouette greater than 0.5 indicates reasonable partitioning of data into appropriate clusters and a value less than 0.2 indicates the data do not exhibit cluster structure [19].

The number of clusters,  $k$ , an input to the k-means algorithm, is decided by the number of dominant eigenvalues of the Laplacian matrix. The silhouette plot is used to confirm the claim that the number of clusters identified using dominant eigenvalues, indeed, provide the best clustering results. Figure 5 shows the eigenvalues plot for the Laplacian matrix used to obtain the preliminary number of clusters as 2. To verify this claim, the clustering procedure is repeated with different number of clusters and the average silhouette value is computed for each case. Table I shows the average silhouette values for clusterings with different number of clusters. The average silhouette value is maximum when the number of clusters is 2, which indicates the natural number of clusters available in the provided data set is 2.

TABLE I  
AVERAGE SILHOUETTE VALUES FOR DIFFERENT CLUSTERING

No.of clusters	2	3	4	5	6	7
Average silhouette value	0.8739	0.8627	0.6409	0.6039	0.6119	0.537

### B. Multiple Operating Conditions

The idea of contingency clustering is extended to account for multiple operating conditions. From the PV analysis, it is found that a maximum of 11.76% of the base load can be increased uniformly at all load buses. For illustration, seven different load levels (3 cases below and above the base load level) have been considered. For example, the load level in scenario S2 is 15% less than that of in S1, whereas the load level in S7 is 6% greater than that of S1. The clustering procedure is repeated at each of the chosen operating conditions.

Table II shows the similarity of different clusterings computed by VOI metric. Theoretically, for the reduced input contingency set, the VOI can have a maximum of 4.3175 for two dissimilar clusterings. The small VOI values in table II indicate that clusterings at different operating conditions being

TABLE II  
SIMILARITY BETWEEN CLUSTERINGS AT DIFFERENT OPERATING  
CONDITIONS USING VOI METRIC

Scenario Load (%)	S1 (Base)	S2 (-15)	S3 (-10)	S4 (-5)	S5 (2)	S6 (4)	S7 (6)
S1	0	0.8652	0.7954	0.3817	0.2052	0.2612	0.4526
S2	0.8652	0	0.6018	0.8727	0.8468	0.8137	0.8534
S3	0.7954	0.6018	0	0.5914	0.8182	0.8087	0.8493
S4	0.3817	0.8727	0.5914	0	0.4628	0.4824	0.6704
S5	0.2052	0.8468	0.8182	0.4628	0	0.1434	0.4109
S6	0.2612	0.8137	0.8087	0.4824	0.1434	0	0.3720
S7	0.4526	0.8534	0.8493	0.6704	0.4109	0.3720	0

similar. In all seven cases, the final number of contingency clusters remain as two. But the number of contingencies in each cluster is different for different cases. At higher load levels, some of the contingencies that are considered as non-severe earlier have become severe and therefore included in the set of identified clusters. For example, S2 has 23 and 28 contingencies in clusters 1 and 2 respectively, as opposed to 29 and 42 in the base case. The change in the number of contingencies between clusterings 1 and 2 has resulted in a VOI of 0.8652. However, the most severe contingencies remains the same at different operating conditions. Therefore, the final set of severe contingencies does not have any new additions compared to the one in base load operating condition. Without loss of generality, the severe contingencies in the base case have been considered for the identification of DVCA.

### C. Dynamic Voltage Control Areas

Results from the contingency clustering analysis provide information about the set of contingencies and buses affected by them. For the modified 162 bus system, the representative contingencies in clusters 1 and 2 results in a violation of 70 buses and they are chosen for further analysis. Although the number of violated buses common to both clusters is high, the severity of the affected buses is different for these two clusters, indicated through the small correlation value ( $SC=-0.3227$ ).

Buses with large KL values corresponding to each representative contingency are selected as the most severely affected buses. Also, it has been observed the most severely affected buses result in performance violations for other contingencies in the corresponding cluster. The contingencies in clusters 1 and 2 result in severe KL performance violations at 44 and 34 buses, respectively. There are 29 buses severely affected only by cluster 1 contingencies and 18 buses severely affected only by cluster 2 contingencies. There are 16 buses severely affected by contingencies in both clusters 1 and 2. Apart from this, there are 8 buses with KL violations for the representative contingencies, but these violations are not severe. Three preliminary DVCA groups are formed by grouping the severely affected buses along with their corresponding contingency clusters. The preliminary DVCA corresponding to the common affected buses includes the contingencies from both clusters.

For the selection of preliminary candidate location using sensitivity studies, 92 load buses in the range of 69-345 kV levels are considered. For each selected potential candidate location, a dynamic VAR source with maximum capacity as 1 p.u, 3 p.u and 5 p.u is placed and the change in the KL measure for each injection level is observed. The different

VAR injection levels are considered to account for the non-linearity in change in KL measure with respect to dynamic VAR injections. The sensitivities of the KL measure with respect to VAR injection at different candidate locations are used to formulate the constraints of the MILP problem as described in section IV-A.

The MILP problem is solved by using a branch and cut search algorithm in CPLEX. This optimization problem identifies the best candidate locations and the amount of dynamic reactive power needed to achieve satisfactory voltage performance, considering all representative contingencies from each cluster. For the representative contingency from each cluster, the MILP chooses 9 candidate locations as optimal locations from the initial set of 92 candidate locations. The chosen control locations that primarily influence the affected buses in preliminary DVCA 1, 2, and 3 are determined 4, 2, and 3, respectively. The control locations corresponding to each preliminary DVCA set along with its influential buses and set of contingencies define the dynamic voltage control area.

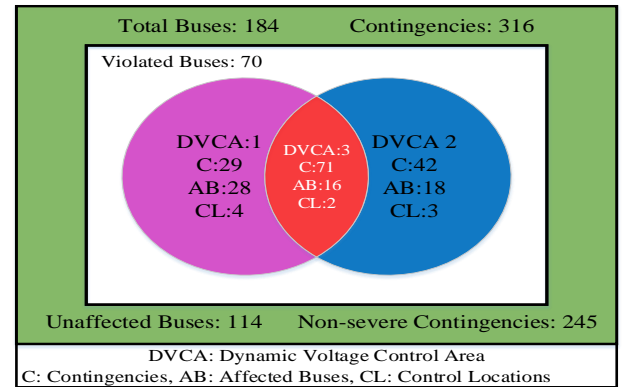


Fig. 10. Summary of DVCA results

Figure 10 shows the summary of the three DVCA for the modified 162 bus system. Each DVCA has three components: (1) set of similarly behaving contingencies, (2) buses affected by this contingency set, and (3) effective control buses that mitigate the problems in the affected buses. DVCA 1 has 29 contingencies, 28 affected buses, and 4 effective control candidate locations. Similarly, 18 buses are severely affected by 42 contingencies in DVCA2 and 3 candidate locations from the 18 affected buses are most effective in mitigating the short-term voltage stability problems. The 16 buses in DVCA3 are affected by both contingencies in DVCA1 and DVCA2, and, therefore, DVCA3 has 71 contingencies. There are 2 control locations in DVCA3 providing dynamic VAR support to the 16 buses in DVCA3 for all the 71 contingencies in DVCA3. As long as the minimum levels of dynamic reactive reserves are maintained in each area, the likelihood of short-term voltage instability is minimized within the corresponding area.

To validate the claim that only representative contingencies are sufficient to perform the MILP optimization, the optimization procedure is repeated with the top 3 contingencies from each cluster set. The MILP optimization yielded the same control candidate locations obtained in the case where only the representative contingencies are used. This approach greatly

reduces the number of dynamic simulations that must be performed, while dealing with multiple contingency analyses during the planning stage.

## VI. CONCLUSIONS

This paper described a clustering based approach for contingency analysis and a novel method for the identification of dynamic voltage control areas. Clustering analysis groups the contingencies based on their similarity patterns of bus responses. The number of contingencies considered for different analyses is greatly reduced, since the severe contingency for each cluster is representative of all other contingencies in this cluster. Also, this approach provides a comprehensive list of contingencies that exposes different weaknesses in the system. The concept of DVCA identifies groups of weak buses vulnerable to short-term voltage problems under a given set of contingencies and also the most effective control locations to provide dynamic reactive support to achieve satisfactory dynamic voltage performance. A MILP optimization problem is formulated to identify effective candidate locations for placing dynamic reactive sources. Identification of DVCA provides information about different regions vulnerable to short term voltage problems, conditions that expose such weakness and locations most effective in mitigating the problem.

## REFERENCES

- [1] M. Chen, "Contingency re-definition and its application to power system security analysis," in *Power Systems Conference and Exposition (PSCE), 2011 IEEE/PES*, 2011, pp. 1–4.
- [2] J. A. Huang, L. Loud, G. Vanier, B. Lambert, and S. Guillon, "Experiences and challenges in contingency analysis at hydro-quebec," in *Power and Energy Society General Meeting, 2012 IEEE*, 2012, pp. 1–9.
- [3] NERC Transmission Issues Subcommittee and System Protection and Control Subcommittee – "Fault-Induced Delayed Voltage Recovery", Technical reference paper, version 1.2, Princeton, NJ, June 2009. [Online]: [http://www.nerc.com/docs/pc/tis/FIDVR\\_Tech\\_Ref%20V1-2\\_PC\\_Approved.pdf](http://www.nerc.com/docs/pc/tis/FIDVR_Tech_Ref%20V1-2_PC_Approved.pdf)
- [4] M. Glavic, D. Novosel, E. Heredia, D. Kosterev, A. Salazar, F. Habibi-Ashrafi, and M. Donnelly, "See it fast to keep calm: Real-time voltage control under stressed conditions," *IEEE Power and Energy Magazine*, vol. 10, no. 4, pp. 43–55, 2012.
- [5] R. Bravo, R. Yinger, D. Chassin, H. Huang, N. Lu, I. Hiskens, and G. Venkataramanan, "Load modelling transmission research - final project report," Lawrence Berkeley National Laboratory,, Tech. Rep., March 2010.
- [6] "Reliability issues risk assessment - Emerging issues survey for long-term reliability assessment," North American Electric Reliability Corporation, Tech. Rep., 2012.
- [7] U. S. Department of Energy Workshop, "On the Role of Residential AC Units in Contributing to Fault-Induced Delayed Voltage Recovery," Westin Dallas Fort Worth Airport, Apr.22, 2008.
- [8] U. S. Department of Energy and NERC, "Fault-Induced Delayed Voltage Recovery Workshop," Sep, 29 2009.
- [9] S. Dasgupta, M. Paramasivam, U. Vaidya, and V. Ajjarapu, "Entropy based analysis of delayed voltage recovery," Accepted for publication in *Transactions on Power Systems*.
- [10] T. M. Cover and J. A. Thomas, *Elements of Information Theory*. New York: Springer, 1991.
- [11] L. K. Nash, *Elements of Statistical Thermodynamics*. Addison-Wesley, 1968.
- [12] D. Shoup, J. Paserba, and C. Taylor, "A survey of current practices for transient voltage dip/sag criteria related to power system stability," in *Power Systems Conference and Exposition, 2004. IEEE PES*, oct. 2004, pp. 1140 – 1147 vol.2.
- [13] U. Luxburg, "A tutorial on spectral clustering," *Statistics and Computing*, vol. 17, no. 4, pp. 395–416, Dec. 2007. [Online]. Available: <http://dx.doi.org/10.1007/s11222-007-9033-z>
- [14] M. Meila, "Comparing clusterings by the variation of information," 2003, pp. 173–187. [Online]. Available: <http://www.springerlink.com/content/rdda4r5bm9ajlbw3>
- [15] K. Morison, X. Wang, A. Moshref, and A. Edris, "Identification of voltage control areas and reactive power reserve: an advancement in on-line voltage security assessment," in *Power and Energy Society General Meeting - Conversion and Delivery of Electrical Energy in the 21st Century, 2008 IEEE*, 2008, pp. 1–7.
- [16] B. Sapkota and V. Vittal, "Dynamic var planning in a large power system using trajectory sensitivities," *Power Systems, IEEE Transactions on*, vol. 25, no. 1, pp. 461 –469, feb. 2010.
- [17] A. Michel, A. Fouad, and V. Vittal, "Power system transient stability using individual machine energy functions," *IEEE Transactions on Circuits and Systems*, vol. 30, no. 5, pp. 266 – 276, 1983.
- [18] Siemens PTI Power Technologies Inc., *PSS/E 33, Program Application Guide, Vol. II, May 2011*.
- [19] L. Kaufman and P. J. Rousseeuw, *Frontmatter*. John Wiley & Sons, Inc., 2008.